Long-range and head-on beam-beam compensation studies in RHIC with lessons for the LHC*

W. Fischer†, Y. Luo, N. Abreu, R. Calaga, C. Montag, G. Robert-Demolaize, BNL,
U. Dorda, J.-P. Koutchouk, G. Sterbini, F. Zimmermann, CERN
H.-J. Kim, T. Sen, V. Shiltsev, A. Valishev, FNAL, J. Qiang, LBNL, A. Kabel, SLAC

Abstract

Long-range as well as head-on beam-beam effects are expected to limit the LHC performance with design parameters. They are are also important consideration for the LHC upgrades. To mitigate long-range effects, current carrying wires parallel to the beam were proposed. Two such wires are installed in RHIC where they allow studying the effect of strong long-range beam-beam effects, as well as the compensation of a single long-range interaction. The tests provide benchmark data for simulations and analytical treatments. Electron lenses were proposed for both RHIC and the LHC to reduce the head-on beam-beam effect. We present the experimental long-range beam-beam program at RHIC and report on head-on compensations studies based on simulations.

INTRODUCTION

Beam-beam effects have limited the performance of previous and existing hadron colliders [1, 2] such as the Sp$\bar{\text{p}}$S [3–6], Tevatron [7–9] and RHIC [10,11], and are also expected to limit the performance of the LHC [12–27].

Beam-beam effects can be categorized as either incoherent (dynamic aperture and beam lifetime), PACMAN (bunch-to-bunch variations), or coherent (beam oscillations and instabilities) [21]. These effects can be caused by both head-on and long-range interactions. Head-on effects, leading to tune shifts and spreads, are important in all hadron colliders. Total beam-beam induced tune shifts as large as 0.028 were achieved in the Sp$\bar{\text{p}}$S [6] and Tevatron [9].

Long-range effects, however, differ in previous and existing colliders. In the Sp$\bar{\text{p}}$S, with both beams in the same pipe and only 3 bunches per beam, there were only a few long-range interactions distributed over the ring circumference, and due to the difference in the bunch intensities, the effect on the antiproton was stronger. In the Tevatron, also with both beams in the same pipe but 36 bunches per beam, there are more long-range interactions, and with the increased intensity of the antiproton bunches, protons can also be affected. In RHIC, where both beams share a pipe only in the interaction regions, there are nominally no long-range beam-beam interactions under store conditions, but long-range interactions have affected the ramp transmission in the past [10]. In the LHC there are 30 long-range beam-beam interactions localized in each of 4 interaction regions [21].

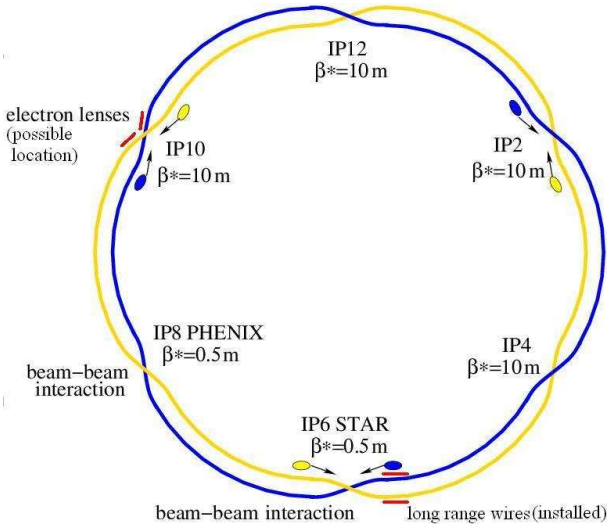

Figure 1: Beam-beam interactions in RHIC and locations of wires and electron lenses. The shown β^* values are for the polarized proton design configuration at 250 GeV, which has not been implemented yet.

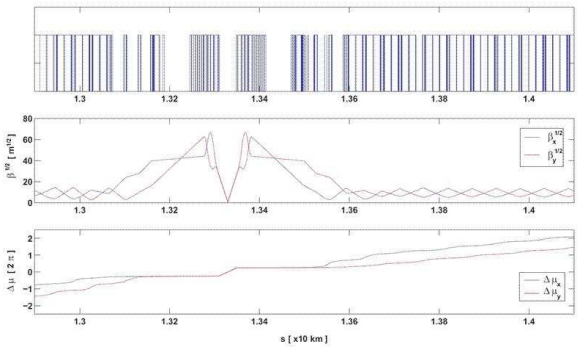

Figure 2: Lattic, β-functions, and phase advances in an LHC interaction region. At location $s = 13.433$ km, with approximately equal horizontal and vertical β-functions, a long-range wire compensator or electron lens could be placed.

* Work supported by US DOE under contract DE-AC02-98CH10886 and the US LHC Accelerator Research Program.

† Wolfram.Fischer@bnl.gov

This work was also supported by the U.S. Department of Energy under Contract No. DE-AC02-05CH11231.

The two main LHC luminosity upgrade scenarios are an early beam separation scheme (ES), and a scheme with a large Piwinski angle (LPA) [22]. In the ES scheme [23, 24] the number of long-range interactions is greatly reduced but 4 parasitic collisions at 4-5 σ remain. In the LPA scheme the small crossing angle will be maintained, and long bunches of intensities up to 4×10^{11} protons are used. The LPA scheme would benefit from long-range beam-beam compensation.

The performance limitation imposed by head-on and long-range beam-beam effects may be ameliorated by beam-beam compensation techniques. Because of the amplitude dependence of the beam-beam forces a proper head-on compensation cannot be done with magnets but requires another particle beam. The compensation of head-on beam-beam effects was first tested in the 4-beam e^+e^- collider DCI [28]. The DCI experience however fell short of expectation because of strong coherent effects [29]. Head-on beam-beam compensation was also proposed for the SSC [30, 31] and the Tevatron [32]. But with most antiprotons now lost through luminosity producing effects, a compensation of the head-on beam-beam effect would not yield more luminosity [9].

The compensation of long-range effects in the Tevatron was proposed with electron lenses [32], and in the LHC with wires [33]. Electron lenses were also considered for the LHC [34], and the use of wires was also studied for the Tevatron [35]. Implementation of long-range beam-beam compensation in the Tevatron is challenging because the effect is distributed over the whole ring. In the LHC the effect is localized in the interaction regions. A partial long-range beam-beam compensation was successfully implemented in the e^+e^- collider DAΦNE [36]. Beam-beam compensation and related issues were reviewed at a workshop in 2007 [37].

Figure 1 shows the basic layout of the beam-beam interaction and compensation studies in RHIC. At store there are nominally 2 head-on interactions in points 6 and 8 (IP6 and IP8), and no long-range interactions. 3 bunches in the Blue ring are coupled to 3 bunches in the Yellow ring through the head-on beam-beam interaction. For studies 2 DC wires were installed in the Blue and Yellow rings respectively in interaction region 6 (IR6). For head-on beam-beam compensation studies in simulations, electron lenses are assumed in IR10. Tab. 1 shows the main beam parameters for polarized proton operation, both achieved and design. In RHIC the beam-beam effect is strongest in proton operation.

In the LHC locations in warm sections of the interactions are reserved to accommodate long-range beam-beam wire compensators (Fig. 2), or electron lenses. These locations have about equal horizontal and vertical β-functions.

Table 1: Main RHIC parameters relevant for beam-beam effects, for polarized protons.

quantity	unit	achieved	design
beam energy E	GeV	100	250
bunch intensity N_b	10^{11}	1.5	2.0
rms emittance ϵ	mm mrad	3.3	3.3
beam-beam parameter ξ/IP	...	0.0056	0.0074
no of IPs	...	2	2
β^* at IP6, IP8	m	1.0	0.5
$(\Delta\psi_x, \Delta\psi_y)_{IP6-IP10}$	π	$(19.1, 19.6)$	
$(\Delta\psi_x, \Delta\psi_y)_{IP8-IP10}$	π	$(8.4, 10.9)$	

LONG-RANGE BEAM-BEAM COMPENSATION STUDIES IN RHIC

With the expected strong long-range beam-beam effects in the LHC, and the proposed wire compensation, experimental data and simulations of long-range effects are desirable. Operational and experimental data exist from the Sp$\bar{p}$S and the Tevatron. In the SPS wires were installed to further investigate strong long-range beam-beam interactions, to test the compensation scheme, and to benchmark simulations [26, 38–40].

The wire experiments in RHIC complement these studies. The beam lifetime in RHIC is typical for a collider and better than in the SPS. In addition, and unlike in the SPS, head-on effects can be included, and with properly placed long-range interactions and wires, the compensation of a single long-range interaction is possible.

Wires in RHIC

The RHIC wire design is based on experience gained with the SPS units. Design considerations are: the location in ring, the integrated strength (IL), the wire temperature T in operation, the positioning range and accuracy, power supply requirements, controls, and diagnostics [41, 42]. The wire parameters are shown in Tab. 2.

Location in the ring. For a successful compensation the phase advance between the long-range interaction and the compensator should be no larger than about 10 degrees [43]. Lattices with $\beta^* \leq 1.0$ m have such small phase advances between the entrance to the DX and the exit of Q3. Thus it is possible to place a wire in the warm region after Q3 to compensate for a long-range beam-beam interaction near the DX magnet (Fig. 3). Since the beam paths must cross horizontally, it is easier to control the distance between the beams in an experiment through vertical separation. To compensate for a vertical long-range interaction near the DX magnet, one wire can be installed in each ring (see Fig. 4). In the Blue ring the wire is installed above the beam axis, in the Yellow ring below the beam axis.

Integrated strength. To compensate a single long-range interaction, the compensator's integrated strength (IL) must be the same as the opposing bunch's current integrated over its length $(IL) = N_b ec$, where I is the cur-

Table 2: Parameters for RHIC wires. The wire material is Cu at 20°C. The nominal wire strength is for a single long-range interaction with a proton bunch intensity of 2×10^{11}.

quantity	unit	value
strength (IL), nominal	A m	9.6
max. strength $(IL)_{max}$	A m	125
length of wire L	m	2.5
radius of wire r	mm	3.5
number of heat sinks n	...	3
electrical resistivity ρ_e	Ω m	1.72×10^{-8}
heat conductivity λ	W m^{-1}K^{-1}	384
thermal expansion coeff.	K^{-1}	1.68×10^{-5}
radius of existing pipe r_p	mm	60
current I, nominal	A	3.8
max. current in wire I_{max}	A	50
current ripple $\Delta I/I$ (at 50 A)	10^{-4}	< 1.7
electric resistance R	mΩ	1.12
max. voltage U_{max}	mV	55.9
max. power P_{max}	W	2.8
max. temp. change ΔT_{max}	K	15
max. length change ΔL_{max}	mm	0.4
vertical position range	mm/σ_y	65/10.6

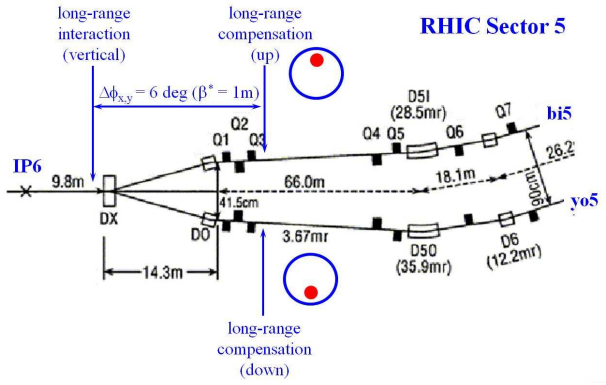

Figure 3: Location of wires in RHIC and location of long-range beam-beam interaction for compensation.

rent in the wire, L its length, N_b the bunch intensity, e the elementary charge, and c the speed of light (see Tab. 2).

In the LHC, an integrated strength of 80 A m is required to correct for the 16 long-range interactions on either side of an IR [33]. Such a strength is also expected to lead to enhanced diffusion at amplitudes larger than 6 rms transverse beam sizes [43]. To study the enhanced diffusion in RHIC, the wire is designed for $(IL)_{max} = 125$ A m.

Wire temperature. The wire's temperature should not exceed 100°C to avoid increased outgassing of the vacuum components. We use $n = 3$ heat sinks cooled with forced air, spaced apart by $L/(n-1)$. The maximum temperature increase in the center between 2 heat sinks is

$$\Delta T_{max} = \frac{1}{8\pi^2}\frac{\rho_e}{\lambda}\frac{(IL)^2}{(n-1)^2 r^4}, \qquad (1)$$

where ρ_e is the electrical resistivity, λ the heat conductivity, and r the wire radius. To move the wire compensator

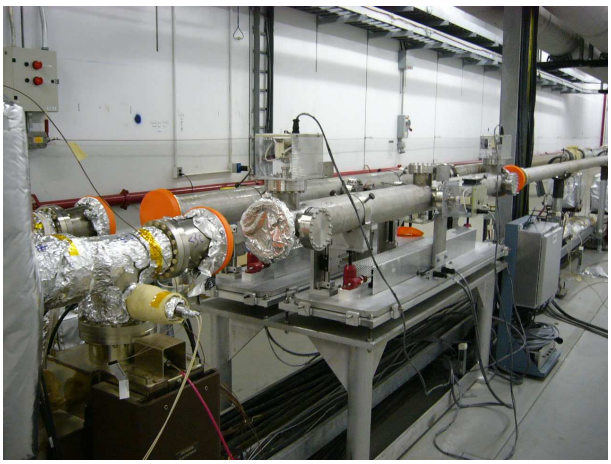

Figure 4: The tow long-range beam-beam wires in the RHIC tunnel during installation.

close to the beam, its radius should not be much larger than an rms transverse beam size. The calculated temperature change with 3 heat sinks is shown in Tab. 2. Fig. 5 shows a drawing of the end of a wire. Visible are the wire support, the electrical feed-through which is also a heat sink, and a connecting loop allowing for thermal expansion of the wire.

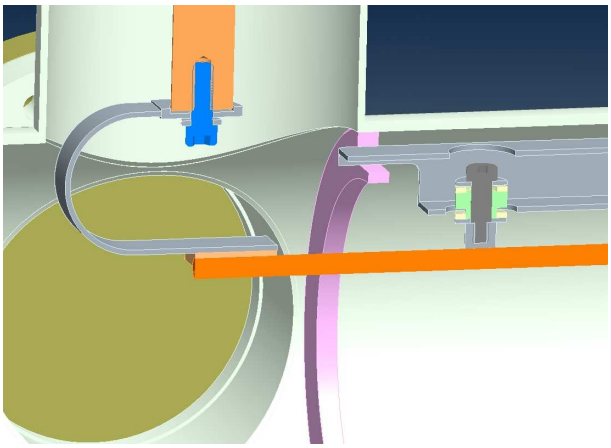

Figure 5: Drawing of the end of a long-range beam-beam wire in RHIC.

Power supply requirements. To limit emittance growth, a current ripple of $\Delta I/I < 10^{-4}$ is required [43]. A measurement shows a current ripple of $\Delta I/I < 1.7 \times 10^{-4}$ where the upper limit is given by the noise floor of the current measurement.

Experiments and simulations

Observables in long-range beam-beam experiments are orbits, tunes, beam transfer functions (BTFs), and the beam lifetime. The main parameters that are varied are the strength of the long-range interactions (wire current), the distance between the beam and the wire (or other beam),

the tune and chromaticity.

Long-range experiments were done with 2 proton beams at injection, 2 proton beams at store, gold beams and wires at store, and deuteron beams and wires at store. All measurements are summarized in Tab. 3. No proton beams have been available for store experiments since the wires were installed. The beam-beam parameter of proton beams is about 3 times larger than the beam-beam parameter of heavy ion beams, and experiments including the head-on effect as well as the compensation of a single long-range interaction are best done with protons. These have not yet been carried out.

Table 4: RHIC parameters for long-range experiments with gold beams at store.

quantity	unit	Blue	Yellow
beam energy E	GeV/n	100	
rigidity $(B\rho)$	T m	831.8	
number of bunches	...	23	
distance IP6 to wire center	m	40.92	
β_x at wire location	m	1091	350
β_y at wire location	m	378	1067

Orbit, tune and chromaticity changes can be calculated as a function of the long-range strength and distance [44], and orbit and tune changes agree with expectations under well controlled experimental circumstances [45, 46]. The beam lifetime, however, is determined through the nonlinear beam-beam effect, and can only be assessed in detailed simulations.

Table 4 shows the main beam parameters for the wire experiments at store with gold beams. Most of the the wire experiments were done with gold beams. Fig. 6 shows a typical scan., In this scan the wire current is set first, and then the distance between the wire and the beam is reduced. Then, at close distance, the wire current is decreased, and again increased. During the scan the beam intensity is recorded, and the beam lifetime can be plotted as a function of the distance between wire and beam. One such plot is shown in Fig. 7.

It was speculated that the beam lifetime τ can be expressed as $\tau = Ad^p$ where A is an amplitude, d the distance between wire and beam, and p an exponent that would typically be in a narrow range. For the SPS τ had been found to be about 5, and for the Tevatron to be about 3 [47]. In Tab. 3 the fitted exponents are listed for all cases for which a fit was possible. The fitted exponents range from 1.7 to 16, i.e. p is not constrained within a narrow range. 10 of the 13 p values are between 4 and 10. Fig. 8 shows the fitted exponents p as a function of the ion tunes in the upper part, and the proton tunes in the lower part. Ion tunes near the diagonal and away from either horizontal or vertical resonances show smaller exponents p. The experiments also showed that the beam lifetime is reduced with increased chromaticity [45].

Another simple measure of assessing the long-range beam-beam effect in experiments is to measure the distance

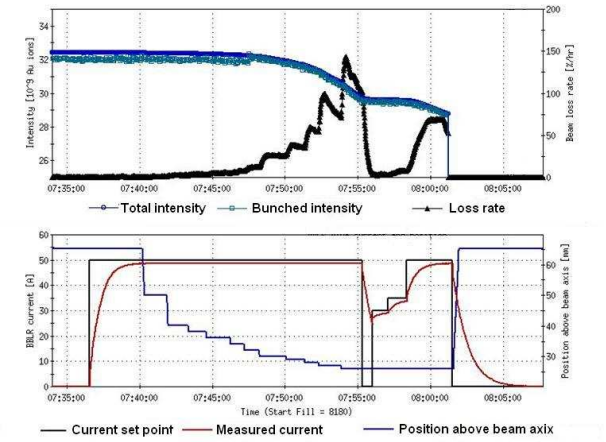

Figure 6: Long-range beam-beam experiment in RHIC with deuteron beam at store. In the upper plot the total and bunched beam intensity is shown (blue curves, left scale) as well as the calculated beam loss rate (black curve, right scale). The lower plot shows the set point for the wire current (black curve, left scale), the measured current (red curve, left scale), and the wire position above the beam pipe center (blue curve, right scale).

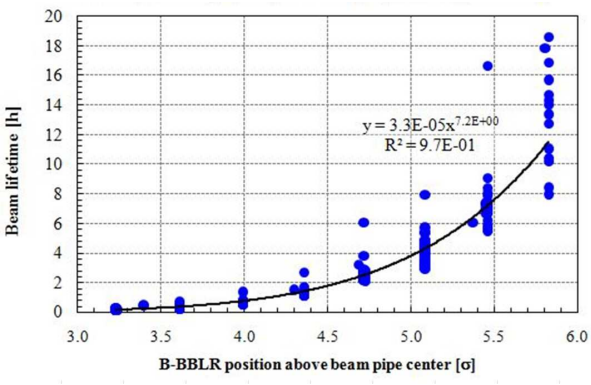

Figure 7: Beam lifetime as a function of the wire position (gold beam at injection, wire strength 125 A m) The lifetime τ is fitted to a function $\tau = Ad^p$.

between the beam and wire (or other beam) at which the beam lifetime become smaller than a certain value. We have chosen this value to be 20 h, which would imply a luminosity lifetime of 10 h or less. Tab. 3 shows an amplitude range between 3.5 and 17 σ. With the limited amount of data no clear correlation can be established between this distance and the fitted coefficient p. In 2 cases the distance was found to be as larger or larger than 10 σ, and most cases fall between 4 and 10 σ. Operation with less than 5 σ separation appears to be difficult [48]. Note that the beam is sometimes used for multiple scans and that a large lifetime drop at large distances is more typical for previously unused beam (Tab. 3).

One important goal of the experiments is to benchmark simulations. In several simulations the onset of large losses

Table 3: Summary of long-range beam-beam experiments in RHIC. The wires in the Blue and Yellow ring are named B-BBLR and Y-BBLR respectively. Fields are left blank when the experimental value could not be determined.

fill no	ring	scan	species	rel. γ	bunches per ring	Q_x	Q_y	LR location	LR strength (IL)	LR separation d	fitted exponent p	d for $\tau < 20$ h	comment
...	...	...	...	...	...	...	...	...	A m	σ	...	σ	
2005													
6981	B	1	p	25.963	1	0.7331	0.7223	IP4	5.3	B moved			weak signal
6981	Y	1	p	25.963	1	0.7267	0.7234	IP4	5.3	B moved			weak signal
6981	B	2	p	25.963	1	0.7351	0.7223	IP4	5.8	B moved			weak signal
6981	Y	2	p	25.963	1	0.7282	0.7233	IP4	5.8	B moved			weak signal
6981	B	3	p	25.963	1	0.7383	0.7247	IR4 DX	8.6	Y moved			weak signal
6981	Y	3	p	25.963	1	0.7271	0.7218	IR4 DX	8.6	Y moved			weak signal
6981	B	4	p	25.963	1	0.7394	0.7271	IR4 DX	8.9	Y moved	4.9	6.5	
6981	Y	4	p	25.963	1	0.7264	0.7388	IR4 DX	8.9	Y moved	2.8		
2006													
7707	B	1	p	106.597	10			IR6 DX	6.7	B moved			weak signal
7707	Y	1	p	106.597	10			IR6 DX	6.7	B moved			weak signal
7707	B	2	p	106.597	10			IR6 DX	6.7	Y moved			weak signal
7707	Y	2	p	106.597	10			IR6 DX	6.7	Y moved			weak signal
7747	B	1	p	106.597	8			IR6 DX	7.9	B moved			weak signal
7747	Y	1	p	106.597	10			IR6 DX	7.9	B moved			weak signal
7747	B	2	p	106.597	8			IR6 DX	7.0	Y moved			weak signal
7747	Y	2	p	106.597	10			IR6 DX	7.0	Y moved			weak signal
7807	B	1	p	106.597	12	0.6912	0.6966	IR6 DX	8.2	Y moved	2.5	3.5	additional octupoles
7807	Y	1	p	106.597	12	0.7092	0.6966	IR6 DX	8.2	Y moved	1.5	3.5	additional octupoles
2007													
8231	B	1	Au	10.520	6	0.2327	0.2141	B-BBLR	12.5	B-BBLR moved	7.2	6.5	
8231	B	1	Au	10.520	6	0.2322	0.2140	B-BBLR	125	B-BBLR moved	7.8	9.0	
8405	B	1	Au	107.369	56	0.2260	0.2270	B-BBLR	125	B-BBLR moved	1.7	15.0	background test
8609	B	1	Au	107.369	23	0.2340	0.2260	B-BBLR	12.5	B-BBLR moved	7.4	6.0	
8609	B	2	Au	107.369	23	0.2340	0.2260	B-BBLR	125	B-BBLR moved	16.0	5.5	
8609	Y	1	Au	107.369	23	0.2280	0.2350	Y-BBLR	12.5	Y-BBLR moved	4.8	9.5	
8609	Y	2	Au	107.369	23	0.2280	0.2350	Y-BBLR	125	Y-BBLR moved	4.1	7.5	
8727	B	1	Au	107.369	23	0.2200	0.2320	B-BBLR	12.5	B-BBLR moved	5.2	9.5	
8727	B	2	Au	107.369	23	0.2200	0.2320	B-BBLR	125	B-BBLR moved	8.1	10.0	
8727	B	1	Au	107.369	23	0.2320	0.2280	Y-BBLR	12.5	Y-BBLR moved	6.3	4.5	
8727	B	2	Au	107.369	23	0.2320	0.2280	Y-BBLR	125	Y-BBLR moved	10.8	5.0	
8727	B	3	Au	107.369	23	0.2320	0.2280	Y-BBLR	125-0	-6.5			
8727	B	4	Au	107.369	23	0.2320	0.2280	Y-BBLR	125	-6.5			ver. chroma 2-8
8727	B	5	Au	107.369	23	0.2320	0.2280	Y-BBLR	125-0	-6.5			ver. chroma 8
2008													
9664	B	1	d	107.369	12	0.2288	0.2248	B-BBLR	125	B-BBLR moved	3.8	17.0	end of physics store
9664	B	2	d	107.369	12	0.2288	0.2248	B-BBLR	75-125	5.8			end of physics store

as a function of the distance between wire and beam was reproduced within about 1 σ [26, 46, 49–51]. One such comparison is shown in Fig. 9.

HEAD-ON BEAM-BEAM COMPENSATION STUDIES IN RHIC

If a collision of a proton beam with another proton beam is followed by a collision with an electron beam, the head-on beam-beam effect can in principle be ameliorated.

Figure 10 shows the layout of a head-on compensation. For simplicity we only consider the horizontal plane and beams with a Gaussian transverse distribution. Before experiencing a beam-beam kick from another ion beam at location 1, a proton has the transverse phase space coordinates (x_0, x_0'). Then the proton receives a kick from the other proton beam [52]

$$\Delta x_0' = \frac{2N_1 r_0}{\gamma x_0}\left[1 - \exp\left(-\frac{x_0^2}{2\sigma_1^2}\right)\right] \qquad (2)$$

where N_1 is the bunch intensity of the other proton beam, γ the relativistic factor of the proton receiving the kick, r_0 the classical proton radius, and σ_1 the rms beam size of the other proton beam. The new coordinates are then

$$x_1 = x_0 \qquad (3)$$
$$x_1' = x_0' + \Delta x_0'. \qquad (4)$$

After transport through the linear beam line the coordinates are

$$x_2 = M_{11}x_1 + M_{12}x_1' \qquad (5)$$
$$x_2' = M_{21}x_1 + M_{22}x_1' \qquad (6)$$

with [53]

$$M_{11} = \sqrt{\frac{\beta_2}{\beta_1}}\left(\cos\Delta\psi + \alpha_1 \sin\Delta\psi\right) \qquad (7)$$
$$M_{12} = \sqrt{\beta_1\beta_2}\,\sin\Delta\psi \qquad (8)$$
$$M_{21} = -\frac{1+\alpha_1\alpha_2}{\sqrt{\beta_1\beta_2}}\sin\Delta\psi + \frac{\alpha_1-\alpha_2}{\sqrt{\beta_1\beta_2}}\cos\Delta\psi \qquad (9)$$
$$M_{22} = \sqrt{\frac{\beta_1}{\beta_2}}\left(\cos\Delta\psi - \alpha_2 \sin\Delta\psi\right) \qquad (10)$$

and $\Delta\psi = \psi_2 - \psi_1$. In the electron lens the proton receives the kick

$$\Delta x_2' = -\frac{2N_2 r_0}{\gamma x_2}\left[1 - \exp\left(-\frac{x_2^2}{2\sigma_2^2}\right)\right] \qquad (11)$$

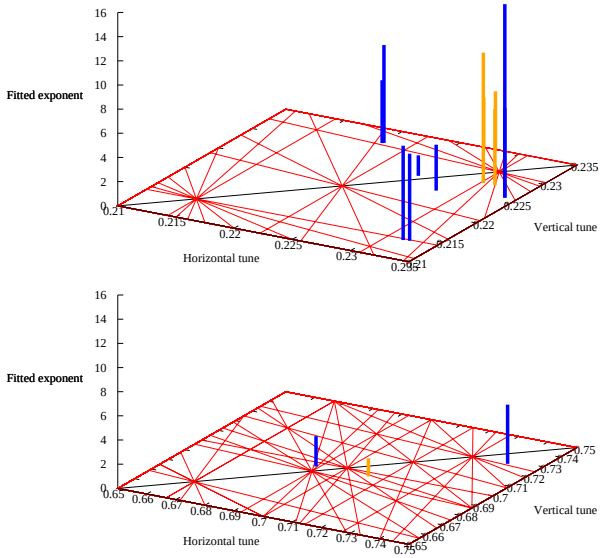

Figure 8: Fitted exponents p for long-range beam-beam experiments as a function of the ion tunes (top) and the proton tunes (bottom). The fitted exponents range from 1.7 to 16.

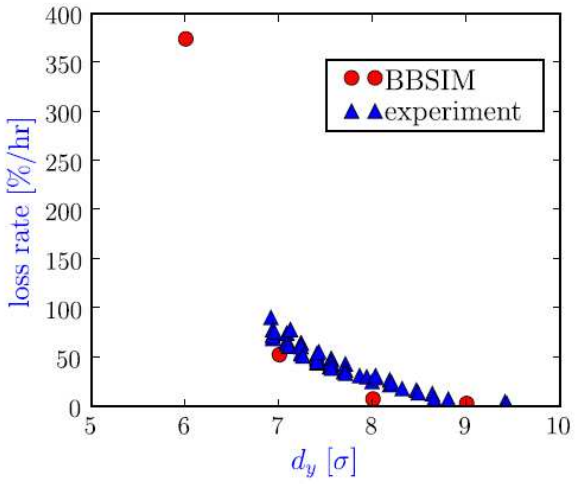

Figure 9: Comparison of measured and simulated beam loss rate as a function of distance between wire and and beam. Experiment with gold beam at store, wire strength of 125 A m [49].

where N_2 is the effective bunch intensity of the electron lens beam (i.e. the number of electrons the proton passes in the lens), and σ_2 the rms beam size of the electron lens beam. The coordinates after passing the electron lens are then

$$x_3 = x_2 \quad (12)$$
$$x_3' = x_2' + \Delta x_2'. \quad (13)$$

One can now express the final coordinates (x_3, x_3') as a function of the intensities (N_1, N_2) and require for exact

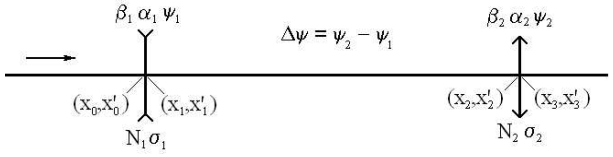

Figure 10: Schematic of head-on beam-beam compensation. At the first location, with lattice parameters $(\beta_1, \alpha_1, \psi_1)$, a proton experiences a beam-beam kick from another proton bunch with intensity N_1 and rms beam size σ_1. At the second location, with lattice parameters $(\beta_2, \alpha_2, \psi_2)$, another beam-beam kick is generated by the electron beam with effective bunch intensity N_2 and rms beam size σ_2.

compensation that

$$x_3(N_1, N_2) = x_3(0,0) \quad \text{and} \quad (14)$$
$$x_3'(N_1, N_2) = x_3'(0,0), \quad (15)$$

i.e. the final coordinates are the same with and without beam-beam interaction and compensation. From the condition (14) it follows that $M_{12} = 0$ and therefore $\Delta\psi = k \cdot \pi$, with k being an integer. From the condition (15) it follows that $N_1 = N_2$ and $\sigma_1^2/\sigma_2^2 = \beta_1/\beta_2$.

Therefore, if the following three conditions are met the beam-beam kicks are canceled exactly:

1. The ion and the electron beam produce the same amplitude dependent force by having the same effective charge and profile.
2. The phase advance between the two beam-beam collisions is a multiple of π in both transverse planes.
3. There are no nonlinearities between the two collisions.

In practice this cannot be achieved, and the goal of the simulation studies is to find out how far one can deviate from these three condition and still expect a sufficiently large increase in the luminosity to make a practical effort of head-on beam-beam compensation worthwhile. With tolerances established one can then assess if these can be achieved with the technology available.

Electron lenses in RHIC

Two electron lenses are currently installed in the Tevatron [54] where they are reliably used as an operational gap cleaner [55]. They were also shown to improve the lifetime of antiproton bunches suffering from PACMAN effects [56]. The experience with the construction and operation of the Tevatron electron lenses provides invaluable input into an assessment of the practicability of head-on beam-beam compensation.

For the RHIC head-on beam-beam compensation studies the electron lenses are assumed to be in IR10 (Fig. 1), at a location that is currently unused. Their parameters (Tab. 5) are assumed to be close to those of the Tevatron electron lenses.

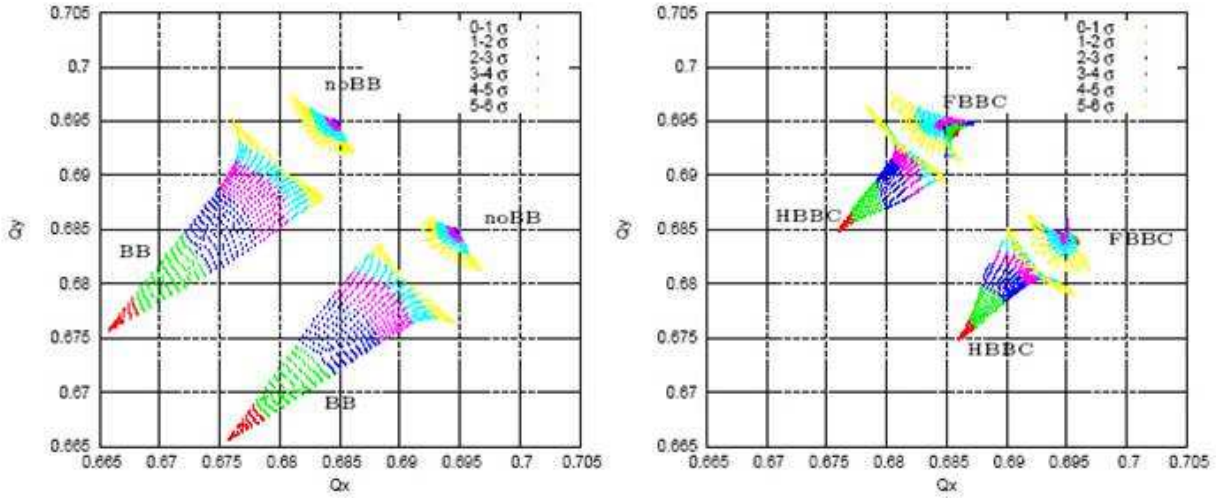

Figure 11: Tune footprints without and with beam-beam interaction (left) as well as with half and full beam-beam compensation (right) [60].

Table 5: Parameters for RHIC electron lenses [57], adapted from the Tevatron electron lenses [54].

quantity	unit	value
electron kinetic energy K_e	keV	5.0
electron speed $\beta_e c$	...	$0.14c$
electron transverse rms size	mm	0.57
effective length L_{elens}	m	2.0
full head-on compensation		
no of electron in lens N_e	10^{11}	3.5
electron beam current I_e	A	1.2

Simulation studies

A number of simplifications are used for the simulations so far. First, the electron lenses are exactly at IP10, while 2 lenses for both beams would need to be installed with a few meters offset from the IP. Second, the electron beam of the electron lens is infinitely stiff (see Refs. [58, 59] for a discussion). Third, a lattice for polarized proton operation at 250 GeV is used with $\beta^* = 0.5$ m in IP6 and IP8, and $\beta^* = 10$ m in all other IPs (see Fig. 1 and Tab. 1). The phase advance in the horizontal plane between IP6 and IP10 is close to a multiple of π, as well as in the vertical plane between IP8 and IP10.

Tune footprints can be compressed with electron lenses (Fig. 11) but this is not sufficient to improve the beam lifetime. At at large compensation compensation strength the tune footprints are folded over which typically leads to reduced stability. The folding can be avoided with a partial compensation.

It was also found that, except for particles at small betatron amplitudes, almost all particles are chaotic (Fig. 12, Ref. [62]), and that therefore chaotic borders cannot be used to evaluate head-on beam-beam problems. Dynamic aperture calculations also proved relatively insensitive since they evaluate the stability of motion at large betatron amplitudes, where the beam-beam forces are small.

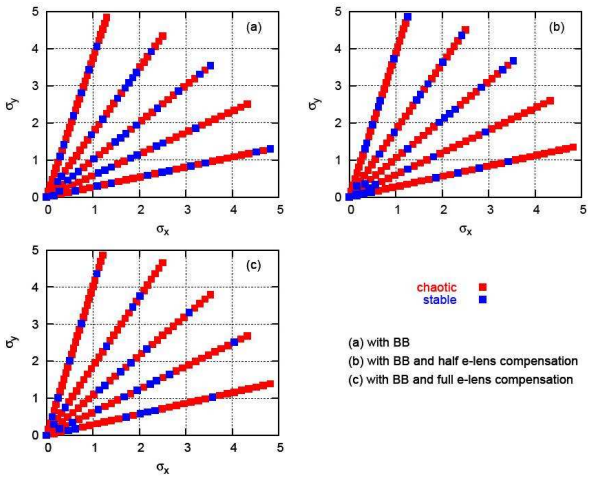

Figure 12: Chaoticity of particle motion with beam-beam interaction, half and full beam-beam compensation. Almost all particles are chaotic. Chaoticity was determined by examining the time evolution over 10^6 turns of the distance of two initially close particles [62].

Other short-term measures calculated were tune diffusion maps (Fig. 13, Ref. [60]), Lyapunov exponent maps (Fig. 14, Ref. [60]), and diffusion coefficients sampled at a number of locations in phase space and fitted with an analytic function (Fig. 15, Ref. [62]). In all these cases we find that the stability of motion is increased at amplitudes below 3 σ and decreased at amplitudes above 4 σ.

In many-particle simulations over a large number of turns with SixTrack the emittance growth was too noisy to to distinguish several cases under study. To distinguish

cases with beam lifetime simulations more than a million turns are necessary, requiring a large amount of CPU time for parameter scans. Beam lifetime simulations are now under way.

The use of electron lenses was also investigated for the head-on beam-beam compensation for the electron beam in the ring-ring version of the electron-ion collider eRHIC [64]. The luminosity of that machine is limited by the beam-beam effect exerted on the electrons. Fig. 16 shows the normalized luminosity as a function of the proton bunch intensity in that machine, calculated in weak-strong simulations. The normalized luminosity is proportional the luminosity for constant electron bunch intensity and collision frequency. With increased proton bunch intensity the luminosity first increases, then decreases again because of the beam-beam effect on the protons that leads to an increase of the core beam size. With half compensation the intensity at which the luminosity decreases can be increased by about a factor 2. An investigation of the transverse tails in the simulation also shows that the proton bunch intensity can be approximately doubled with an electron lens. From these weak-strong simulations we therefore expect about a factor 2 increase in luminosity from the beam-beam compensation.

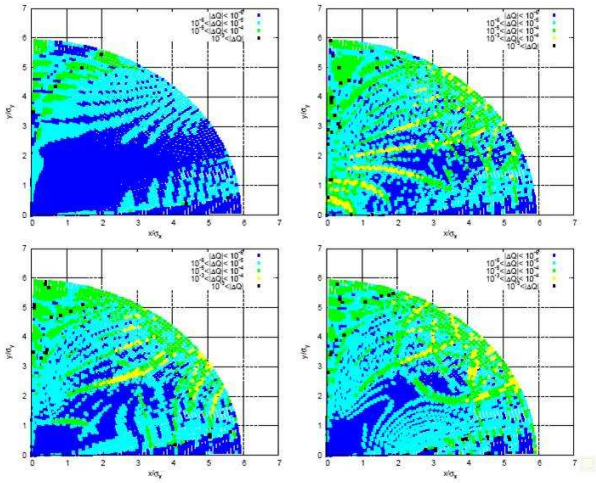

Figure 13: Tune diffusion without beam-beam interaction (top left), with beam-beam interaction (top right), with half (bottom left), and with full beam-beam compensation [60].

SUMMARY

Long-range beam-beam experiments were carried out in RHIC with 2 DC wires parallel to the beam. These experiments complement experience with long-range beam-beam interactions in the Sp$\bar{\text{p}}$S and Tevatron, and wire experiments in the SPS. The RHIC wires can create strong localized long-range beam-beam effects, comparable in strength to the effect expected in the LHC, with a beam that has a lifetime typical of hadron colliders and possibly including head-on beam-beam collisions.

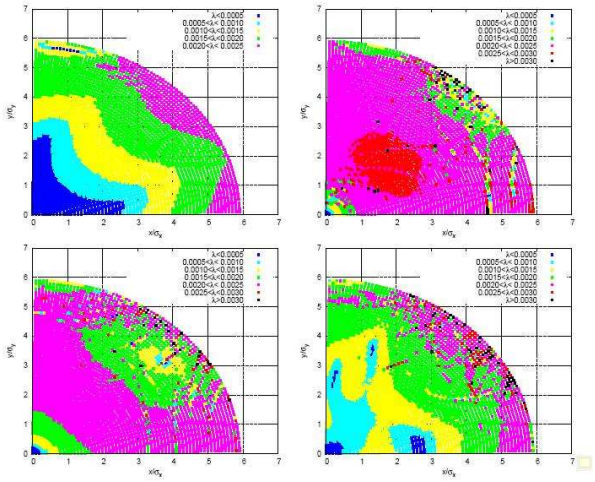

Figure 14: Lyapunov exponents without beam-beam interaction (top left), with beam-beam interaction (top right), with half (bottom left), and with full beam-beam compensation [60].

The RHIC experiments confirmed that a visible effect of long-range beam-beam interactions should be expected, although their effect sensitively depends on a number of beam parameters such as the tune and chromaticity. Fitting the beam lifetime τ to an exponential function $\tau \propto d^p$ as a function of the distance d between the beam and the wire, exponents p in the range between 1.7 and 16 were found. The experimentally observed distance from the wire to the beam at which large beam losses set in could be reproduced in simulations within 1 σ. Distances smaller than 5 σ appear to be problematic to maintain good beam lifetime.

Long-range wire experiments with protons, and including the head-on effect, are still outstanding.

In simulations for head-on beam-beam compensation in RHIC, short-term measures such as diffusion maps, Lyapunov exponent maps and action diffusion coefficients all show an increase of the stability for betatron amplitudes below 3 σ, and a reduction of stability for amplitudes larger than 4 σ. This is particularly pronounced for full head-on compensation and suggests to use partial compensation only. For full compensation the tune footprints are already folded over at small amplitudes.

In operation there are only few particles beyond 4 σ, and whether the decreased stability at these amplitudes can be tolerated can be estimated in beam lifetime and emittance growth simulations over up to 10^7 turns with 10^4 macroparticles. These simulations should also test the sensitivity to a number of parameters, including the phase advance between the beam-beam interaction and the electron lens, and orbit errors at the electron lens location. The latter was found to be of critical importance in the Tevatron electron lens operation.

Electron lenses were also studied in weak-strong simulations to compensate the head-on beam-beam effect on the electrons in the ring-ring version of the electron-ion

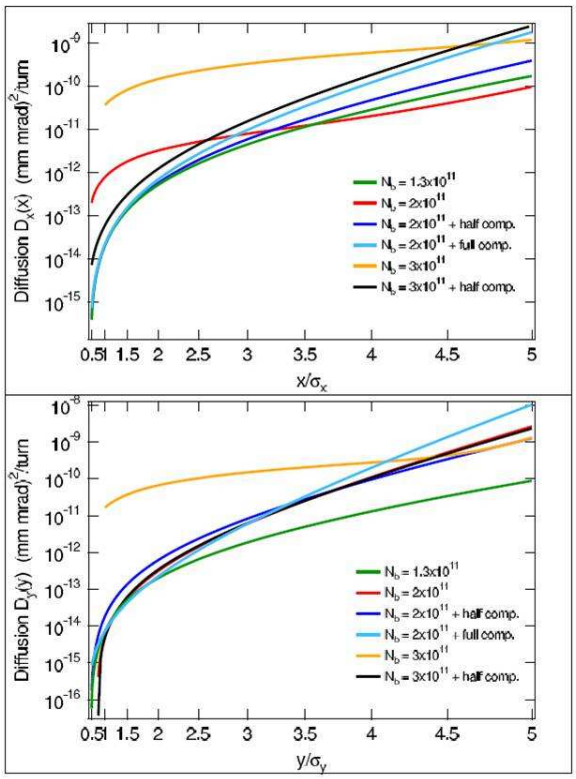

Figure 15: Fitted diffusion coefficient for different bunch intensities and with half and full beam-beam compensation [62].

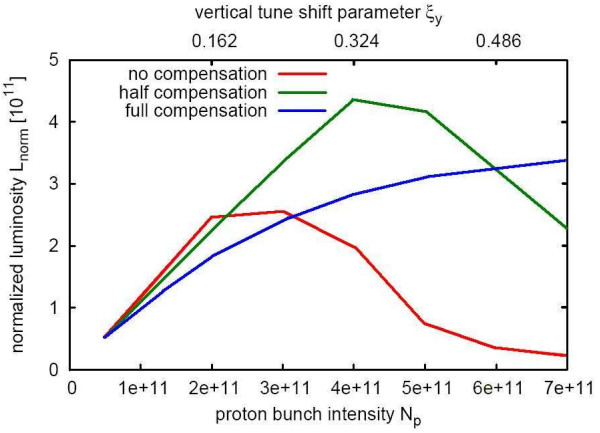

Figure 16: Normalized luminosity in the eRHIC ring-ring version as a function of the proton bunch intensity without, with half and with full head-on beam-beam compensation [64].

collider eRHIC [64]. From these simulation a luminosity increase of about a factor two is expected from the beam-beam compensation.

ACKNOWLEDGMENTS

For discussions and help we are most thankful to collaborators within the US LHC Accelerator Research Program as well a several people at various laboratories. Among these are Y. Alexahin, E. Beebe, J. Beebe-Wang, O. Brüning, R. DeMaria, W. Herr, V. Kamerdzhiev, E. McIntosh, C. Milardi, K. Ohmi, M. Okamura, A. Pikin, T. Pieloni, F. Schmidt, and S. Tepikian.

REFERENCES

[1] E. Keil, proceedings PAC'89, pp. 1731-1735 (1989).
[2] Y. Alexahin, proceedings PAC'05, pp. 544-548 (2005).
[3] L.R. Evans and J. Gareyte, proceedings PAC'83, pp. 2397-2399 (1983).
[4] L. Evans, J. Gareyte, M. Meddahi, R. Schmidt, proceedings PAC'89, pp. 1403-1405 (1989).
[5] K. Cornelis, M. Meddahi, R. Schmidt, proceedings EPAC'90, pp. 1670-1672 (1990).
[6] K. Cornelis, proceedings LHC'99, CERN-SL-99-039 AP (1999).
[7] X. Zhang, T. Sen, V. Shiltsev, M. Xiao, Y. Alexahin, F. Schmidt, F. Zimmermann, proceedings PAC'03, pp. 1757-1759 (2003).
[8] V. Shiltsev, Y. Alexahin, V. Lebedev, P. Lebrun, R. S. Moore, T. Sen, A. Tollestrup, A. Valishev, and X. L. Zhang, Phys. Rev. ST Accel. Beams 8, 101001 (2005).
[9] A. Valishev, proceedings EPAC'08, pp. 2937-2941 (2008).
[10] W. Fischer, M. Blaskiewicz, J.M. Brennan, P. Cameron, R. Connolly, C. Montag, S. Peggs, F. Pilat, V. Ptitsyn, S. Tepikian, D. Trbojevic, and J. van Zeijts, proceedings PAC'03, pp. 135-137 (2003).
[11] V. Ptitsyn et al., proceedings EPAC'06, pp. 592-594 (2006).
[12] W. Herr, proceedings PAC'91, pp. 1068-1070 (1991).
[13] N. Gelfand, C. Johnstone, T. Sen, and W. Wan, proceedings PAC'99, pp. 1677-1679 (1999).
[14] J. Gareyte, proceedings LHC'99, CERN-SL-99-039 AP, pp. 28-32 (1999).
[15] M.A. Furman and W.C. Turner, proceedings EPAC'00, pp. 1196-1189 (2000).
[16] H. Grote, proceedings EPAC'00, pp. 1202-1204 (2000).
[17] L.H.A. Leunissen, H. Grote, and F. Schmidt, proceedings EPAC'00, pp. 1208-1210 (2000).
[18] M.P. Zorzano and T. Sen, proceedings EPAC'00, pp. 1226-1228 (2000).
[19] M.P. Zorzano and F. Zimmermann, proceedings EPAC'00, pp. 1229-1231 (2000).
[20] W. Herr, proceedings EPAC'00, pp. 1630-1632 (2000).
[21] O. Brüning, P. Collier, P. Lebrun, S. Myers, R. Ostojic, J. Poole, P. Proudlock (editors), CERN-2004-003 (2004).
[22] F. Zimmermann, proceedings PAC'07, pp. 714-718 (2007).
[23] J.-P. Koutchouk, proceedings PAC'07, pp. 3387-3389 (2007).
[24] G. Sterbini and G. Tommasini, proceedings EPAC'08, pp. 2461-2463 (2008).
[25] K. Ohmi, proceedings EPAC'08, pp. 2593-2595 (2008).
[26] U. Dorda, PhD thesis, Vienna University of Technology, Austria (2008).

[27] T. Pieloni, PhD thesis, Ecole Polytechnique Federale de Lausanne, Switzerland (2008).

[28] G. Arzelia et al., Proc. 8th Int. Conf. High Energy Acc., pp. 150 (1971).

[29] M. Bergher et al., proceedings PAC'79, pp. 3559-3561 (1979).

[30] E. Tsyganov, R. Meinke, W. Nexsen, A. Zinchenko, SSCL-PREPRINT-519 (1993).

[31] E. Tsyganov, E. Tarantin, A. Zinchenko, JINR-E9-96-4 (1996).

[32] V. Shiltsev, V. Danilov, D. Finley, and A. Sery, Phys. Rev. ST Accel. Beams 2, 071001 (1999).

[33] J.-P. Koutchouk, proceedings PAC'01, pp. 1681-1683 (2004).

[34] U. Dorda, F. Zimmermann, W. Fischer, and V. Shiltsev, proceedings PAC'07, pp. 1589-1591 (2007).

[35] T. Sen and B. Erdelyi, proceedings PAC'05, pp. 2645-2647 (2005).

[36] C. Milardi, D. Alesini, M.A. Pregner, P. Raimondi, M. Zobov, and D. Shatilov, proceedings EPAC'06, pp. 2808-2810 (2006).

[37] W. Fischer, O. Brning, J.-P. Koutchouk, F. Zimmermann, T. Sen, V. Shiltsev, K. Ohmi, M. Furman, Y. Cai, and A. Chao, informal note BNL C-A/AP/291; ICFA Beam Dynamics Newsletter No. 44, pp. 220-225; proceedings of BEAM'07, CERN-2008-005, CARE-Conf-08-004-HHH (2008).

[38] J.-P. Koutchouk, J. Wenniger, and F. Zimmermann, proceedings EPAC'04, pp. 1936-1938 (2004).

[39] F. Zimmermann, J.-P. Koutchouk, F. Roncarolo, J. Wenninger, T. Sen, V. Shiltsev, Y. Papaphilippou, proceedings PAC'05, pp. 686-688 (2005).

[40] U. Dorda, J.-P. Koutchouk, R. Tomas, J. Wenniger, F. Zimmermann, R. Calaga, and W. Fischer, proceedings EPAC'08, pp. 3176-3178 (2008).

[41] W. Fischer, R. Alforque, H.C. Hseuh, R. Lambiase, C.J. Liaw, G. Miglionico, T. Russo, J.-P. Koutchouk, F. Zimmermann, and T. Sen, informal note BNL C-A/AP/236 (2006).

[42] W. Fischer, R. Calaga, U. Dorda, J.-P. Koutchouk, F. Zimmermann, V. Ranjbar, T. Sen, J. Shi, J. Qiang, and A. Kabel, proceedings EPAC'06, pp. 2158-2160 (2006).

[43] F. Zimmermann, proceedings of the Beam-Beam Workshop at Fermilab, FERMILAB-Conf-01/390-T, CERN LHC Project Report 502 (2001)

[44] T. Sen and B. Erdelyi, proceedings EPAC'02, pp. 1247-1249 (2004).

[45] W. Fischer, N. Abreu, R. Calaga, G. Robert-Demolaize, H.-J. Kim, T. Sen, J. Qiang, A.C. Kabel, U. Dorda, J.-P. Koutchouk, and F. Zimmermann, New Mexico, pp. 1859-1861 (2007).

[46] H.J. Kim and T. Sen, proceeding PAC'07, pp. 3492-3494 (2007).

[47] F. Zimmermann, private communication.

[48] N. Abreu, proceedings BEAM'07, CERN-2008-005, CARE-Conf-08-004-HHH (2008)

[49] H.J. Kim, T. Sen, N.P. Abreu, and W. Fischer, proceedings HB2008 (2008).

[50] H.J. Kim, T. Sen, N.P. Abreu, and W. Fischer, proceedings EPAC'08, pp. 3119-3121 (2008).

[51] A. Kabel, private communication.

[52] E. Keil, CERN 95-06, pp. 539-555 (1995).

[53] D.A. Edwards and M. Syphers, in "Handbook of accelerator physics and engineering", 3rd printing, World Scientific, p. 65 (2006)

[54] V. Shiltsev et al., Phys. Rev. ST Accel. Beams 11, 103501 (2008).

[55] X.-L. Zhang, K. Bishofberger, V. Kamerdzhiev, V. Lebedev, V. Shiltsev, R. Thurman-Keup, and A. Tollestrup, Phys. Rev. ST Accel. Beams 11, 051002 (2008).

[56] V. Shiltsev, Y. Alexahin, K. Bishofberger, V. Kamerdzhiev, G. Kuznetsov, and X.-L. Zhang, Phys. Rev. Lett. 99, 244801 (2007).

[57] Y. Luo and W. Fischer, informal note BNL C-A/AP/286 (2007).

[58] V. Shiltsev and A. Zinchenko, Phys. Rev. ST Accel. Beams 1, 064001 (1998).

[59] A. Burov, V. Danilov, and V. Shiltsev, Phys. Rev. E 59, 3605 (1999).

[60] Y. Luo, W. Fischer, and N. Abreu, BNL C-A/AP/310 (2008), submitted to Phys. Rev. ST Accel. Beams.

[61] Y. Luo, W. Fischer, N. Abreu, E. Beebe, J. Beebe-Wang, C. Montag, M. Okamura, A. Pikin, and G. Robert-Demolaize, proceedings EPAC'08, pp. 328-330 (2008).

[62] N.P. Abreu, W. Fischer, Y. Luo, and G. Robert-Demolaize, proceedings EPAC'08, pp. 2521-2523 (2008).

[63] Y. Luo, G. Robert-Demolaize, N. Abreu, and W. Fischer, proceedings EPAC'08, pp. 3125-3127 (2008).

[64] C. Montag and W. Fischer, submitted to Phys. Rev. ST Accel. Beams. (2008).

[65] U. Dorda, F. Caspers, T. Kroyer, and F. Zimmermann, proceedings EPAC'08, pp. 3173-3175 (2008).

[66] U. Dorda and F. Zimmermann, proceedings EPAC'08, pp. 2245-2247 (2006).

[67] J. Qiang, W. Fischer, and Tanaji Sen, proceedings PAC'07, pp. 3979-3981 (2007).

[68] V. Shiltsev et al., proceedings PAC'05, pp. 2083-2085 (2005).